We appreciate the valuable comments and suggestions that greatly helped us improve our work. You will find point by point responses addressing all the issues in the following text.

Answers to Referee #1's general comments:

1) The emissions retrieved in this study are expressed by the amount of a pollutant in unit volume (μg m^{-3} h^{-1} or ppbv h^{-1}). The dimension of such expression is different from the one used in normal inventories (the amount of a pollutant in unit area, e.g, μg m^{-2} h^{-1} or molecules m^{-2} h^{-1}). Note that for some elevated sources (e.g., stacks or aircraft) in an inventory, the altitude range information is generally given when the emission rates have a unit of μg m-3 h-1 or ppbv h-1. Therefore, the emission rates derived in this study can neither be used directly into the model nor compared quantitatively with previous emission inventories. To convert their retrieved emission rates into the normal ones, the authors need to state clearly to what altitude range their emission rates apply.

Thank you for your constructive advice. The reason why we did not convert the units into one that is conventional for inventories is that we did not want to introduce extra uncertainty into the calculation. In the conversion, planetary boundary layer heights (PBLH) across the domain are required, which would bring up modelling errors of the PBLH. However, we agree that the unit poses a problem for the direct comparison between our results and other inventories and raises confusion. Hence, we decided to make the conversion of the unit in the following way:

Instead of using the measured volume concentrations as C_l in eq.5 ($\overline{E}_{mn} = \overline{\sum_{l=1}^{M} W_{mn} \cdot C_l / T_l}^{mn}$), we replace C_l by a planetary boundary layer column mass concentration in units of $\mu g \cdot m^{-2}$. This would result in a derived $\overline{E}_{mn}$ in the unit of $\mu g \cdot m^{-2} \cdot hr^{-1}$. To bring it to unison with typical inventories, the emission field is multiplied by the area (A_{mn}) of the respective grids (m,n) , yielding a concentration field in the unit of $\mu g \cdot hr^{-1} \cdot cell^{-1}$:

$$\overline{E}_{mn} = \overline{\sum_{l=1}^{M} W_{mn} \cdot C_l \cdot A_{mn} / T_l}^{mn} \quad (1).$$

During daytime, in the convective boundary layer (CBL), we can assume that pollutants are well mixed and concentrations are the same throughout the CBL. After sunset until the early morning, under the stable boundary layer (SBL), pollutant concentrations are assumed to decrease exponentially with height. Typically, the quasi-stationary CBL has been build up in the late morning and collapses late in the afternoon, during sunset. Since in our observation period, the sunrise time lies between 4:55 a.m. and 05:11 a.m., and the sunset time varies from 07:40 p.m. to 07:09 p.m., the

daytime period was defined as 9 a.m. to 6 p.m.

For CO, the original measurements are given as mixing ratio (γ_{CO}) in *ppbv*, thus the column concentration in the CBL can be calculated as is shown in eq.(2):

$$C_l = \frac{\gamma_{CO} \cdot M_{CO} \cdot P}{R \cdot T} \cdot PBLH \quad (2),$$

where M_{CO} is the molar concentration of CO, P and T respectively stand for the atmospheric pressure and temperature and R is the ideal gas constant. In the SBL, C_l is calculated as:

$$C_l = \frac{\gamma_{CO} \cdot M_{CO} \cdot P}{R \cdot T} \cdot \int_{z=0}^{\infty} e^{-\frac{z}{PBLH}} dz \quad (3).$$

BC measurements are given as mass concentrations (m_{BC}) in $\mu g \cdot m^{-3}$, thus the column mass in the CBL and SBL can be respectively calculated according to eq. (4)-(5).

$$C_l = m_{BC} \cdot PBLH \quad (4)$$

$$C_l = m_{BC} \cdot \int_{z=0}^{\infty} e^{-\frac{z}{PBLH}} dz \quad (5)$$

BC and CO emissions mostly come from sources within the boundary layer, to which our derived results apply. Direct comparisons with the INTEX-B inventory or other inventories can then be made by converting the unit from $Ton \cdot year^{-1} \cdot cell^{-1}$ to $\mu g \cdot hr^{-1} \cdot cell^{-1}$ ($1 Ton \cdot year^{-1} \cdot cell^{-1} = 10^{12}/365/24$ $\mu g \cdot hr^{-1} \cdot cell^{-1}$).

2) It is confusing whether the method could be used for regional emission retrieval (independent of previous inventories) or it could be used only for regional emission update (dependent of previous inventories). Sometimes they stated this method of emission retrieval is straightforward, but finally they had to use INTEX-B inventory as the first guess fields. As can been in Fig. 4a2 and b2, the emission rates retrieved for most of land areas are comparable to the false values derived for the sea areas, indicating that there can be large errors in the retrieved source strength and distributions.

We appreciate the questions and helpful comments. A few alterations have been made to improve our method. After these alterations, our method was definitely able to retrieve regional emissions on its own, showing very little dependence on the a priori field. Details on the alterations are discussed below, new retrieval results can be found in Sect. 3.2 in the revised manuscript.

The first modification has already been discussed in 1).

Secondly, the modelling of the high resolution meteorology field was performed again, with a larger

outer domain and with another planetary boundary layer scheme. Since we are discussing emissions and transport of pollutants within the PBL, it is very important that the modelling can capture well the motion and development of meteorological parameters in the boundary layer. The former simulations were performed with WRF version 2, while our new model results are given by a version 3 WRF model. The PBL physics were parameterized using the Yonsei University scheme, which in many assessments have been proven to be the best performing parameterization scheme, especially during summer (Hu et al., 2010, García-Díez et al., 2011). The modelled PBL height is illustrated as the blue line in fig. 1. As you can see, the PBLH during the night reaches a very low level (~30m) and shows no temporal variations. This phenomenon has been observed for all the modelled days, which indicates that this PBL scheme is weak in modelling the night time boundary layer. In the modelling results of WRF version 3, improvements can be seen, but the nocturnal boundary layer still seems to be very low. Wu et al. (2011) has evaluated 4 PBL schemes in WRF 3.2, results also show that all PBL schemes generally do well in unstable and weak stable boundary layers, but poor in stable boundary layer. In their evaluation, the YSU scheme does overall slightly better than other three, for which reason we decided to keep using this scheme. However, we have kept in mind that the low stable boundary layers may result in some bias.

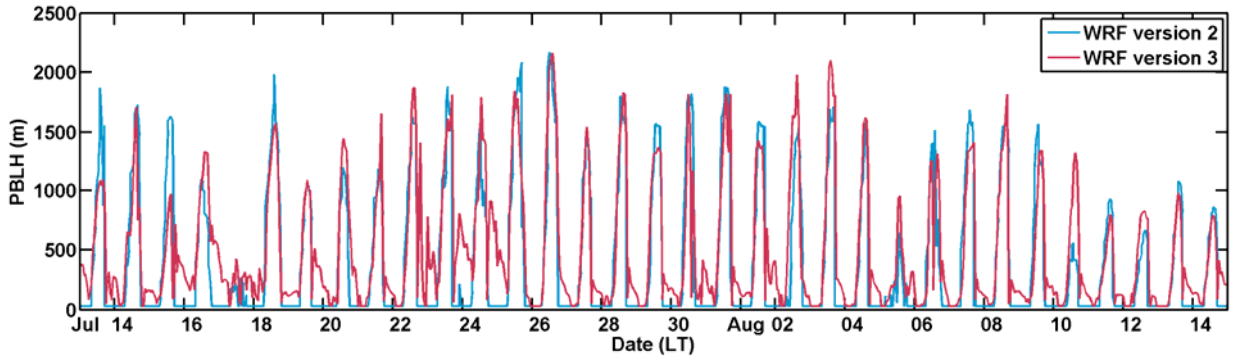

Figure 1. Modelling results of the PBLH at Wuqing.

Since the new meteorology modelling results can provide a more reasonable variation of the PBLH, the WRF PBLH field is employed to determine the residence time, which is our third alteration. As you can see in Figure 2a), the daytime PBLH was assumed to be 1000m and the nighttime PBLH was set at 300m. The residence time is the time difference between the starting time and the time point at which the trajectory exceeds the PBLH. In our new calculations, we applied WRF PBLH values instead of fixed assumed ones. The PBLH values associated with each time point t_i and grid point *(m,n)* over which trajectory *l* passes is sorted out and then used to determine when the trajectory flow exceeds the boundary layer height.

Another change has been made concerning the weighting factor that is used in former eq.5 (now eq.(1)). Since comparisons to the INTEX-B inventories are made, it seems inappropriate and also

unconvincing to use those as weighting factors. Also the INTEX-B inventory might not be the best a priori guess, since the inventory has been made in 2006 and North China Plain has undergone rapid developments since then. Instead, we applied the average MODIS AOD (Atmospheric Optical Depth) distribution, because it can reflect to a certain extent the distribution of aerosol columnar loading. We also did the same retrieval with the average distribution of OMI NO_2 tropospheric column as weighting factor. Both aerosol and NO_2 are rather short-lived in the atmosphere, suggesting that their distributions are closely related to emissions.

After these alterations, our method was able to retrieve regional emissions on its own, retrieval results not using any weighting factor are almost the same as those using either AOD or NO2 as weighting factor. Theoretically, the method would be improved by applying a weighting factor, because it compensates for the assumption that concentrations along the same trajectory are the same. However, it is not dependent too much on the factor itself, as long as the weighting factor is chosen appropriately.

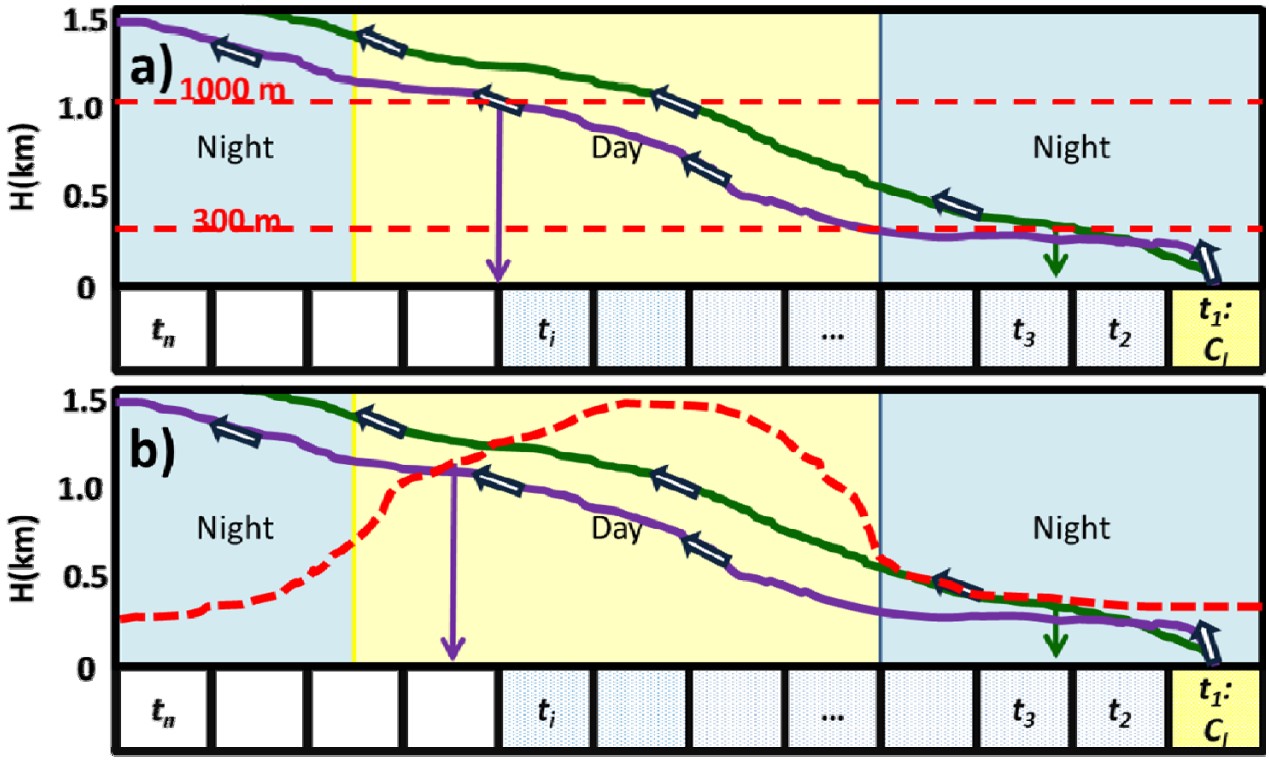

Figure 2. a) Schematic showing the determination of the PBL residence time of trajectories (Figure 2 in ACPD paper), b) New determination method of the PBL residence time.

Reference

García-Díez, M., Fernández, J., Fita, L., and Yagüe, C.: WRF skill over Europe with 3 PBL schemes during the year 2001, 3rd International Meeting on Meteorology and Climatology of the Mediterranean, 2011.

Hu, X.-M., Nielsen-Gammon, J. W., and Zhang, F.: Evaluation of Three Planetary Boundary Layer Schemes in the WRF Model, Journal of Applied Meteorology and Climatology, 49, 1831-1844, 10.1175/2010jamc2432.1, 2010.

Wu, W., Liu, Y., Vandenberghe, F., Bourgeois, A., Grim, J., Warner, T., Knievel, J., Dudhia, J., Bruyere, C., Stauffer, D., Padovani, M., Luft, G., and Fling, K.: Evaluating PBL Schemes in WRF3.2, WRF workshop, 2011.

3) The retrieving procedure is not well demonstrated in the manuscript. Instead of presenting the results directly (Fig. 4), the authors need to show their methods and results step by step. First, how could the positions of the important sources e.g., cities and large steel pants, be located, and then how could their emission rates be calculated? Are these estimating steps coupled together?

Thank you for your advice. Accordingly, we improved the demonstration of the retrieval. A step by step process from the local measurements to the final retrieval of the emission field is provided in our revised manuscript.

Since our method is based on statistical analysis, the retrieval only provides the total emission on each grid. It does not directly provide the positions of important sources and cannot differentiate between the different sources of the same pollutant. However, as is shown in Zhang et al.(2009), the share of emissions by each sector (transportation, residential, industry and power) has changed little during 2000-2006. Thus, a rough estimate could be made on the emission of different sources using their share of emissions as provided by the INTEX-B or other inventories. However, since this is not the purpose of our work, it will only be briefly mentioned in the revised manuscript.

Reference

Zhang, Q., Streets, D. G., Carmichael, G. R., He, K. B., Huo, H., Kannari, A., Klimont, Z., Park, I. S., Reddy, S., Fu, J. S., Chen, D., Duan, L., Lei, Y., Wang, L. T., and Yao, Z. L.: Asian emissions in 2006 for the NASA INTEX-B mission, Atmos. Chem. Phys., 9, 5131-5153, 10.5194/acp-9-5131-2009, 2009.

4) The uncertainties and limitations of their estimate method should be discussed in detail. For example, are there any biases in the estimated positions of the important sources (cities and large

power, steel and coke plants), or these important source positions are pre-described? What are the uncertainties or confidence of their emission rate estimates? Considering both INTEX-B inventory and the method developed in this study may have large bias, the authors need to provide strong evidence to support that at least for some cities or some grids they could update the emission estimates for the year 2009.

We thank the reviewer for the good questions. To answer them, another section (Sect. 3.4) is added to "Results and Discussions", featuring the uncertainty discussion on local measurements, WRF PBLH, wet deposition parameterization, trajectory calculation, etc. More details are also discussed later in the specific comments.

Answers to Referee #1's specific comments:

1) Page 31138, Line 14, what does 'reasonable emission' mean? Line 15-20, these results are meaningless for emission estimates.

With "reasonable emission" we want to express that the derived results show a similar distribution as previous results, yet it also captured some changes in the emission distribution, e.g. the elevated emissions in Tianjin and NE Hebei.

Page 31138, Line 15-20 discusses the results from the concentration contribution assessments, which is part of the application of our method. Indeed, it has nothing to do with deriving emissions, but it shows that we can apply the derived emissions to assessing the contributions from surrounding areas to our receptor site, which is important for the establishment of air quality management strategies. However, we agree that the detailed results of the assessment do not need to appear in the abstract part.

2) Page 31140, does m or n refer to the same variable in the Eqs. (1) and (2)?

Thank you very much for noticing. The m and n on Page 31140 are respectively referring to the total number of endpoints falling within a certain grid and the subset of endpoints that are on trajectories associated with concentrations above a certain criterion. To avoid the confusion with the symbols, Eq. (1) has been modified to $PSCF(m,n) = \frac{t(m,n)}{T(m,n)}$.

3) Page 31141, Line 15-21, what are the biases of CO and BC measurements?

The CO measurements were conducted using the 48C-series gas filter correlation analyser from Thermo Environmental Instruments. The instrument has a lower detection limit of 0.04 ppm, a zero noise of 0.02 ppm and a precision of ±0.1 ppm (Lin et al., 2009). The zero drift for 24hours is below 0.1 ppm, automatic zero checks were conducted every 6 hours. The linearity of the multipoint calibrations showed R2 in the range of 0.9993 and 0.9998, with a 3% variation in linear slope.

BC mass concentrations were calculated using the measured absorption coefficients (σ_{ap}) from the MAAP instrument according to $\sigma_{ap}=m_{BC}\cdot 6.6 m^2/g$, where $6.6 m^2/g$ is the mass absorption efficiency Ma et al. (2011). The uncertainty in σ_{ap} measured by MAAP was estimated to be below 12 % (Petzold and Schönlinner, 2004; Petzold et al., 2005).

The above information was added to Sect. 3.4 (Uncertainties of derived emissions).

Reference:

Lin, W., Xu, X., Ge, B., and Zhang, X.: Characteristics of gaseous pollutants at Gucheng, a rural site southwest of Beijing, J. Geophys. Res., 114, D00G14, 10.1029/2008jd010339, 2009.

Ma, N., Zhao, C. S., Nowak, A., Müller, T., Pfeifer, S., Cheng, Y. F., Deng, Z. Z., Liu, P. F., Xu, W. Y., Ran, L., Yan, P., Göbel, T., Hallbauer, E., Mildenberger, K., Henning, S., Yu, J., Chen, L. L., Zhou, X. J., Stratmann, F., and Wiedensohler, A.: Aerosol optical properties in the North China Plain during HaChi campaign: an in-situ optical closure study, Atmos. Chem. Phys., 11, 5959-5973, 10.5194/acp-11-5959-2011, 2011.

Petzold, A., and Schönlinner, M.: Multi-angle absorption photometry—a new method for the measurement of aerosol light absorption and atmospheric black carbon, Journal of Aerosol Science, 35, 421-441, 10.1016/j.jaerosci.2003.09.005, 2004.

Petzold, A., Schloesser, H., Sheridan, P. J., Arnott, W. P., Ogren, J. A., and Virkkula, A.: Evaluation of Multiangle Absorption Photometry for Measuring Aerosol Light Absorption, Aerosol Science and Technology, 39, 40-51, 10.1080/027868290901945, 2005.

4) Page 31142, Line 1-3 and Fig. 1, the two domains have nearly the same area.

Thank you for pointing that out. In the WRF simulations, the outer domain was only applied to provide a better boundary condition for the inner domain and to downsize the horizontal resolution with a 1 to 3 ratio. In the trajectory analyses, only the inner domain was considered. To spare computational time, the outer domain was chosen to be not far larger than the inner one.

However, we agree that the unconventional outer domain setup of ours may not be able to provide the inner domain with optimal boundary values. To avoid any possible errors it might bring, we altered the size of the outer domain to 2 times the size of the inner domain (fig. 3).

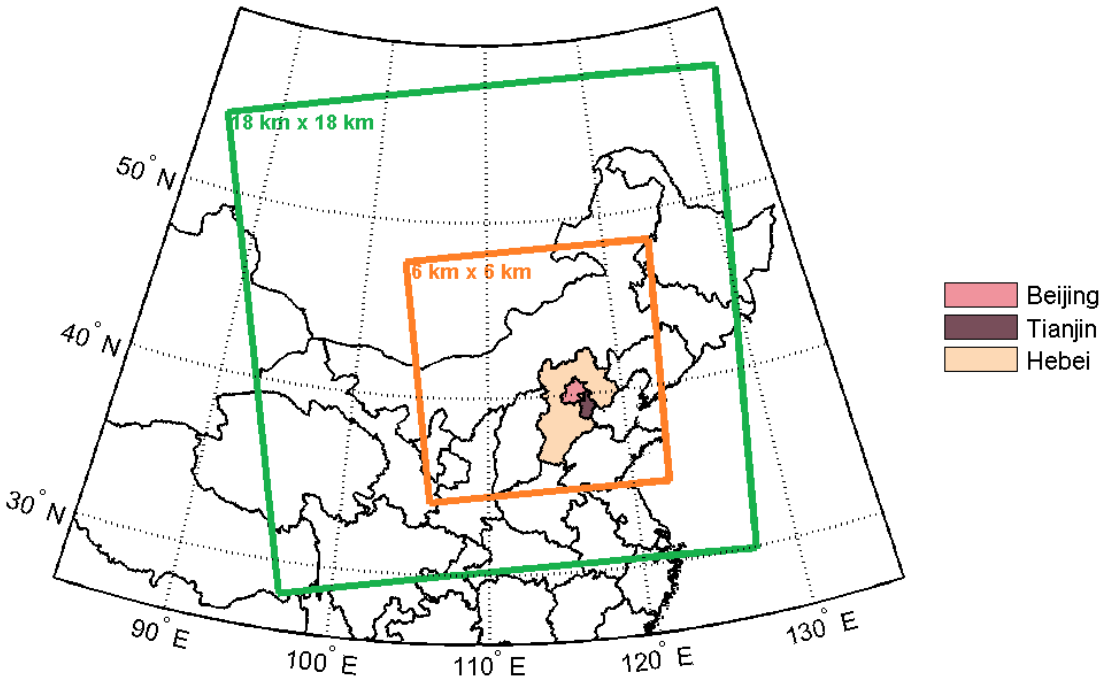

Figure 3. Model domains for the ARW meteorology simulations

5) Page 31143, Line 3-8 and Eq. (3), Could other processes, e.g., deposition and dilution, affect the Ci? Were there any cloudy and rainy days during the experiment period? It is difficult to understand the pollutant concentrations and emission rates ('factor') could be the same for all grids on the same trajectory, especially in the case when a city is in the middle way.

The transport of pollutants in the atmosphere is affected by many factors, surely including dilution and deposition processes or even chemical processes. However, within a certain range of time, we may assume that some processes have rather weak influences. The influence of dilution, dry and wet deposition will be discussed below. We came to the conclusion that wet deposition should be taken into account for BC, for CO wet deposition will have negligible influences, however, to make our method adaptable for other gases, a wet deposition parameterization has also been added.

But first, to respond to the last comment, the weighting factor introduced in our method should compensate for the fact that concentrations are evenly attributed to the whole trajectory. Also trajectories are intersecting each other on the grids, attributing multiple emission values to the same grid. The more samples we have on each grid, the less are the uncertainties brought up by such an assumption.

1. **Dilution:** The effect of dilution on C_l may be of importance under large winds, which only occur

during rain events in summer. It is however not considered in our manuscript, due to its complexity, and would theoretically result in an underestimation of emissions. However, the effect of dilution is implicitly included in our method. Under large winds, trajectories experience shorter residence times, which makes up for the underestimate according to eq(1).

2. **Dry deposition:** CO has a molar mass of 28 g/mol, which is close to the molar mass of air, thus CO is not influenced by dry deposition. Black Carbon aerosols (BC) are mostly submicron particles with sizes of 0.3-0.4μm (Yu et al., 2010, Hitzenberger and Tohno, 2011), which are part of the accumulation mode (0.05-2μm). Ultrafine particles (<0.05μm) are transported to the quasi-laminar layer by Brownian diffusion, larger particles (2-20μm) depend on inertia impaction. For accumulation mode particles, both effects are weak and inefficient (fig. 4). Thus dry deposition for BC can be ignored.

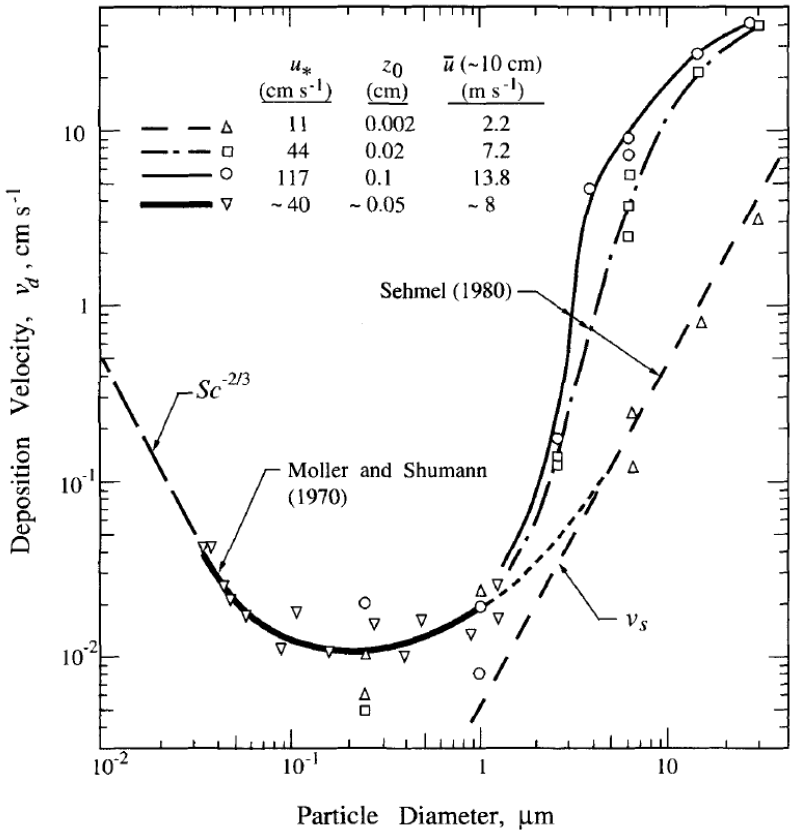

Figure 4. Particle dry deposition velocity data for deposition on a water surface in a wind tunnel (Slinn et al. 1978)

3. **Wet deposition:** CO, with a solubility of 27.6 mg/L (25°C), is only weakly soluble in water. According to Henry's law:

$$[CO(aq)] = H_{CO} \cdot P_{CO} = H_{CO} \cdot \gamma_{CO} \cdot P \quad (6),$$

where $[CO(aq)]$ is the aqueous phase concentration of CO (mol·L^{-1}) in raindrops, H_{CO} is the Henry's law coefficient for CO (H_{CO}=1600 M·atm^{-1}, Sander, 1999) and P_{CO} is the partial

pressure of CO in the atmosphere (atm). Assuming that all the CO that went into aqueous phase fell together with the raindrops to the ground, then the total amount of scavenged CO (in column mass concentration, g·m^{-2}) can be estimated as:

$$C_{CO,wet} = [CO(aq)] \cdot 10^{3} \cdot M_{CO} \cdot P_r \cdot 10^{-3} = H_{CO} \cdot \gamma_{CO} \cdot P \cdot M_{CO} \cdot P_r \quad (7),$$

where M_{CO} is the molar mass of CO, P_r (mm) is the hourly average precipitation amount over a unit area (1 m^2). To avoid using the mixing ratio that is probably already influenced by precipitation, we calculate the wet deposition amount with the γ_{CO} that was observed an hour earlier than each precipitation record.

Results are given in fig. 7d). As you can see, the fraction of scavenged CO column concentration is below 3·10^{-4} %, fully proving the fact that wet scavenging can be ignored for CO. However, if our method should be applied to other trace gases, that are more soluble, e.g. SO_2, a wet deposition correction is required.

First local column concentrations of gas *a* have to be corrected for wet deposition:

$$C_a^{'} = C_a + C_{a,wet} = \begin{cases} (1 + H_a \cdot P_r \cdot R \cdot T / PBLH) \cdot C_a , & 9a.m. \le hr \le 6p.m \\ (1 + H_a \cdot P_r \cdot R \cdot T \Big/ \int_{z=0}^{\infty} e^{-\frac{z}{PBLH}} dz) \cdot C_a , & hr < 9a.m. \; or \; hr > 6p.m \end{cases} \quad (8).$$

By defining a wet scavenging correction coefficient in the form of:

$$k_{wet}^{a} = \begin{cases} (1 + H_a \cdot P_r \cdot R \cdot T / PBLH) , & 9a.m. \le hr \le 6p.m \\ (1 + H_a \cdot P_r \cdot R \cdot T \Big/ \int_{z=0}^{\infty} e^{-\frac{z}{PBLH}} dz), & hr < 9a.m. \; or \; hr > 6p.m \end{cases} \quad (9),$$

the corrected column mass concentration can be obtained by:

$$C_a^{'} = k_{wet}^{a} \cdot C_a . \quad (10)$$

Column concentrations along the track also need to be corrected with the wet scavenging correction coefficient for all grids *(m,n)* that trajectory *l* travels through:

$$\overline{E}_{mn} = \overline{\sum_{l=1}^{M} W_{mn} \cdot k_{wet,mn}^{a} \cdot C_{a,l}^{'} \cdot A_{mn} / T_l}^{mn} = \overline{\sum_{l=1}^{M} W_{mn} \cdot k_{wet}^{a} \cdot k_{wet,mn}^{a} \cdot C_{a,l} \cdot A_{mn} / T_l}^{mn} , \quad (11)$$

where $k_{wet}^{a} = \begin{cases} (1 + H_a \cdot P_{r,mn} \cdot R \cdot T_{mn} / PBLH_{mn}) , & 9a.m. \le hr \le 6p.m \\ (1 + H_a \cdot P_{r,mn} \cdot R \cdot T_{mn} \Big/ \int_{z=0}^{\infty} e^{-\frac{z}{PBLH_{mn}}} dz), & hr < 9a.m. \; or \; hr > 6p.m \end{cases}$. (12)

Ultrafine particles easily come into contact with raindrops through Brownian diffusion, while larger particles are easily caught by raindrops through impaction and interception. Those two

effects are weak for the accumulation mode particles (fig. 5), which mainly depend on acting as CCN (cloud condensation nuclei) and developing into cloud drops to get scavenged from the atmosphere. However, BC aerosols are hydrophobic particles that are not soluble in water, thus are mostly CCN-inactive (Kuwata and Kondo, 2008). Aged BC aerosols are often coated with water soluble substances, which make them more hydrophilic. Wet scavenging coefficients for water soluble particles are often parameterized in the form of $k_s = a \cdot Pr^b$, with a in the range of 0.36 to 1.28 and b in the range of 0.64 to 0.78 (Constantin, 2004). If we want to apply such a parameterization, we have to know the fraction of core-shell BC that can be wet deposited (f_{wet}).

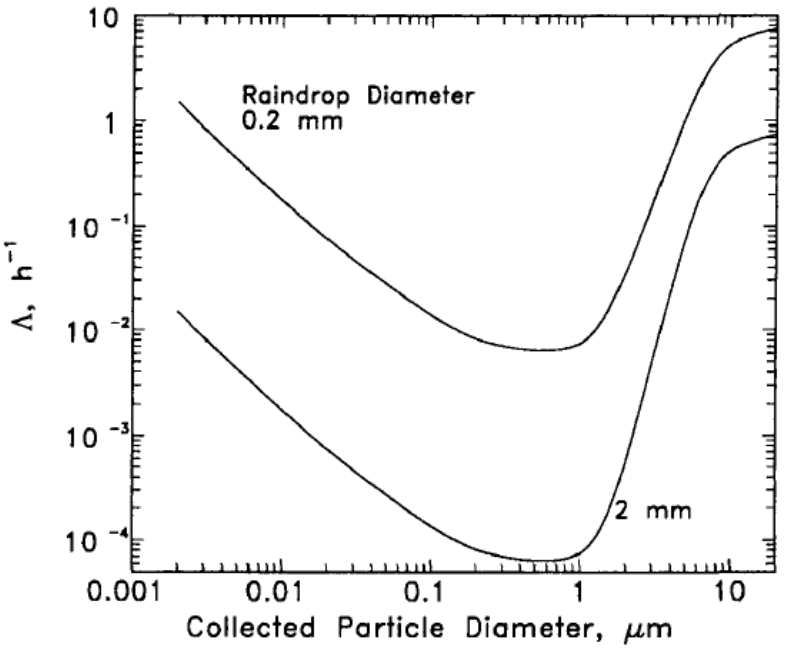

Figure 5. Scavenging coefficient for monodisperse particles as a function of their diameter collected by monodisperse raindrops with diameters 0.2 and 2 mm assuming a rainfall intensity of 1 mm·h^{-1} (Seinfeld & Pandis, 2006).

North China Plain is abundant in highly hygroscopic particles (Liu et al., 2011), thus thinly coated BC particles have rather small chances in becoming activated or washed out. Shiraiwa et al. (2007) investigated the evolution of the mixing state of BC in Tokyo and found out that during polluted days, the number fraction of thickly coated BC particles ranged from 0.07 to 0.42, revealing a clear diurnal cycle that is low during the night and higher during the day. The assumption we make for the diurnal variation of f_{wet} is shown in fig.6.

The final parameterization of BC wet scavenging is applied as:

$$C_{BC,wet} = f_{wet} \cdot k_s^{BC} \cdot C_{BC} = f_{wet} \cdot a \cdot Pr^b \cdot C_{BC} \quad (13)$$

Similar to the wet deposition correction of CO, the correction for BC is given as:

$$C'_{BC} = C_{BC} + C_{BC,wet} = (1 + f_{wet} \cdot a \cdot Pr^{b}) \cdot C_{BC} = k_{wet}^{BC} \cdot C_{BC} \quad (14),$$

$$\overline{E}_{mn} = \overline{\sum_{l=1}^{M} W_{mn} \cdot k_{wet,mn}^{BC} C'_{BC,l} \cdot A_{mn} / T_l}^{mn} = \overline{\sum_{l=1}^{M} W_{mn} \cdot k_{wet}^{BC} \cdot k_{wet,mn}^{BC} \cdot C_{BC,l} \cdot A_{mn} / T_l}^{mn} \quad (15),$$

with k_{wet}^{BC} being the wet scavenging correction coefficient for BC at the receptor point and $k_{wet,mn}^{BC}$ the correction coefficient for the grids trajectory *l* passes through. The parameters *a* and *b* in eq. (13)-(14) are set as 0.8 and 0.7, respectively.

Results of local BC wet scavenging are displayed in fig. 7f). The maximum scavenged BC mass concentration reached 0.5 μg·m^{-3} and the fraction of wet scavenged BC in the total BC mass concentration ($\frac{m_{BC,wet}}{m_{BC} + m_{BC,wet}}$) can reach up to 17.9%, suggesting that wet deposition has a certain influence on BC concentrations and thus also on the retrieval results.

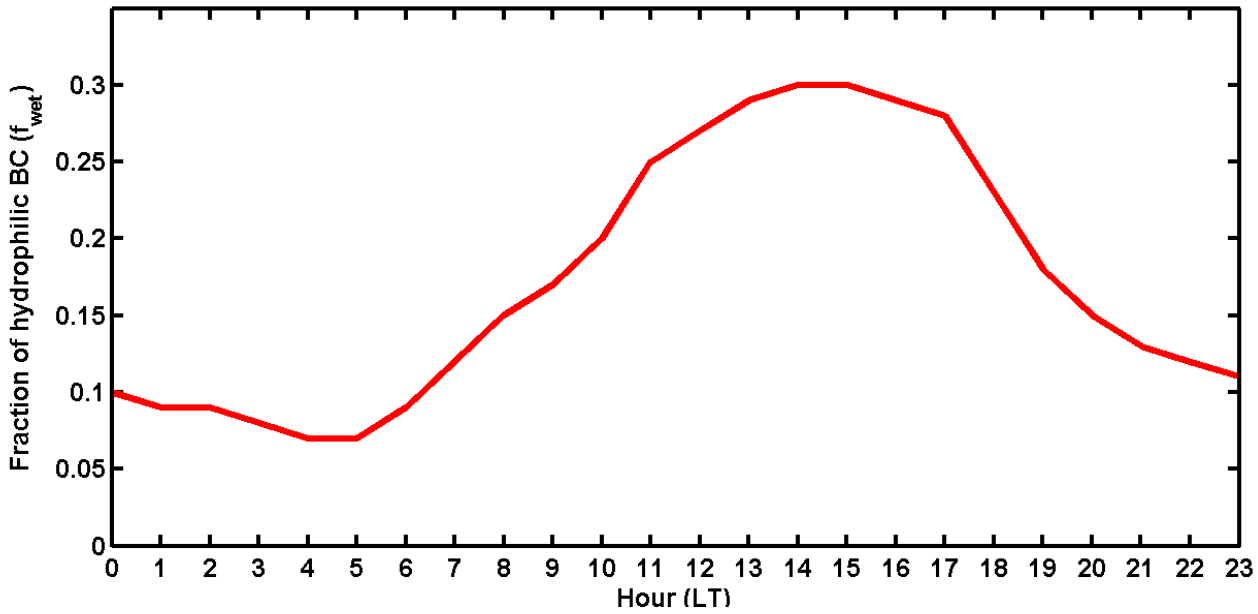

Figure 6. Assumed diurnal cycle of hydrophilic BC particle fraction.

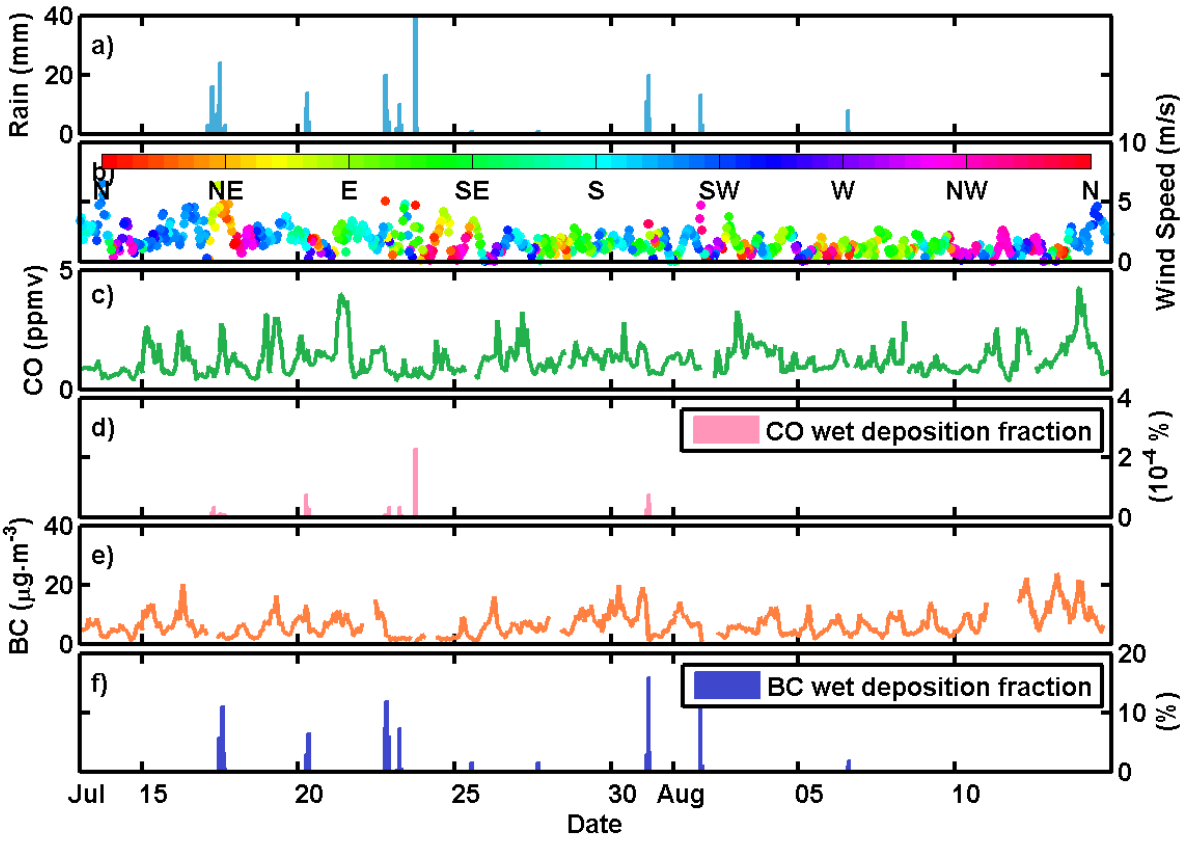

Figure 7. Evaluating the effect of wet deposition on CO and BC. a) Hourly accumulated Precipitation amount. b) Hourly average wind speed and wind direction. c) Hourly average CO mixing ratio. d) Calculated wet deposited CO column mass concentration fraction. e) Hourly average BC mass concentration. f) Calculated wet scavenged BC column mass concentration fraction.

Reference

Constantin, A.: Estimates of sulfate aerosol wet scavenging coefficient for locations in the Eastern United States, Atmospheric Environment, 38, 795-804, 10.1016/j.atmosenv.2003.10.035, 2004.

Hitzenberger, R., and Tohno, S.: Comparison of black carbon (BC) aerosols in two urban areas – concentrations and size distributions, Atmospheric Environment, 35, 2153-2167, 10.1016/s1352-2310(00)00480-5, 2001.

Kuwata, M., and Kondo, Y.: Dependence of size-resolved CCN spectra on the mixing state of nonvolatile cores observed in Tokyo, J. Geophys. Res., 113, D19202, 10.1029/2007jd009761, 2008.

Liu, P. F., Zhao, C. S., Göbel, T., Hallbauer, E., Nowak, A., Ran, L., Xu, W. Y., Deng, Z. Z., Ma, N., Mildenberger, K., Henning, S., Stratmann, F., and Wiedensohler, A.: Hygroscopic properties of aerosol particles at high relative humidity and their diurnal variations in the North China Plain, Atmos. Chem. Phys., 11, 3479-3494, 10.5194/acp-11-3479-2011, 2011.

Sander, R.: Compilation of Henry's Law Constants for Inorganic and Organic Species of Potential Importance in Environmental Chemistry (Version 3), http://www.henrys-law.org, 1999.

Seinfeld, J. H. and S. N. Pandis: Atmospheric Chemistry and Physics - from air pollution to climate change, Hoboken, New Jersey, John Wiley & Sons, Inc, 2006.
Shiraiwa, M., Kondo, Y., Moteki, N., Takegawa, N., Miyazaki, Y., and Blake, D. R.: Evolution of mixing state of black carbon in polluted air from Tokyo, Geophys. Res. Lett., 34, L16803, 10.1029/2007gl029819, 2007.
Slinn, W. G. N., Hasse, L., Hicks, B. B, Hogan, A. W., Lai, D., Liss, P. S., Munnich, K. O., Sehmel, G. A., and Vittori, O.: Some aspects of the transfer of atmospheric trace constituents past the air-sea interface, Atmos. Environ. , 12, 2055-2087, 1978.
Yu, H., Wu, C., Wu, D., and Yu, J. Z.: Size distributions of elemental carbon and its contribution to light extinction in urban and rural locations in the pearl river delta region, China, Atmos. Chem. Phys., 10, 5107-5119, 10.5194/acp-10-5107-2010, 2010.

6) Page 31143, Line 9-13 and Eq. (4), do these multiple emission values represent the real situation, or they are just the uncertainties caused by the method itself?

The multiple emission values on each grid are representative of both the variation of the emissions from day to day and the uncertainty of calculated trajectories. The uncertainty in trajectories may result in misplaced emission values, adding to the standard deviation of the emission value on each grid. The temporal variation of emissions also can lead to various emission values appearing on the same grid. Differentiating the standard deviation caused by those two effects is not possible yet.

7) Page 31143, Line 13-23 and Eqs. (5) and (6), it is unbelievable that the field of any variables could serve as a priori to the emission field analyses. If they think so, the authors should show that the retrieved results from different fields can be neglected.

We agree that not "any variable" can serve as a priori to the emission field analyses. The weighting factor should definitely be a variable that is fully representative of the distribution of emissions. The original sentence is replaced by:

"Considering that is might be unrealistic to assume that all grids on l have the same emission rate, especially when l travels a long distance and crosses the path of large emission sources, the method can be improved by introducing a weighting factor W:

$$W_{mn} = \frac{F_{mn}}{\overline{F}_{mnl}} \qquad (5),$$

where F should be the field of variables that are closely related to the distribution of emissions and can serve as a priori to the emission field analyses, e.g. population, NO_2 column distribution,

aerosol optical depth distribution or previous emission inventories. $\overline{F}_{mnl}$ *is the average value of F for the grids (m,n) that l travels over.*"

As already mentioned in the response to the General comments no. **2**, instead of using the INTEX-B inventory as the *F*, we use the average AOD and NO_2 column distribution as a priori.

8) Page 31144, Line 1-9, Eq. (7) and Fig. 2, how much could the variation in the PBL affect the emission estimates? The PBL height can be much less than 1000m in the morning and much higher than 1000m in the afternoon.

The PBLH assumptions in the previous method determines the residence time, thus having two effects.

1. An underestimation of PBLH would reduce the coverage of the derived emission field, because once the trajectory height exceeds the PBL height, it will not be taken into account anymore.
2. An underestimation in PBLH would give shorter residence time, which results in higher emission estimates according to eq.3 ($\overline{E}_{mn} = \overline{\sum_{l=1}^{M} C_l / T_l}^{mn}$) in the previous manuscript.

In our new method, PBLH is also used to calculate C_l, an underestimation in PBLH would result in the underestimation of C_l and thus a lower emission estimate.

To minimize the uncertainty brought on by the assumption of the boundary layer height, the PBLH in the WRF meteorology simulations are employed. The impact of the uncertainty of the PBLH on the emission estimates are evaluated in the revised manuscript in Sect. 3.4.2.

9) Table 1, how about the sample numbers and standard deviations? Are the values for Tianjin and Beijing comparable to the INTEX-B inventory?

Each grid has at least 5 valid samples. The standard deviations are shown in Table 1 in the revised manuscript.

After modifying our retrieval method, the derived emissions can be directly compared with the INTEX-B inventory (see Sect. 3.2 in the revised manuscript). The values are comparable but higher than those given by the INTEX-B inventory, which is understandable given the rapid economic development and the fast expanding population in the North China Plain. Table 3 has been added listing the average, minimum and maximum standard deviations in various sectors.

10) Figs. 3 and 4, for which grids the emission rates can be updated according to the meteorological conditions during the experiment period and the uncertainties of the method?

That is a good question. The aim of our work is mainly to provide a simple however robust method for emission retrieval. Derived emissions may bear uncertainties of various factors, but with the development of the atmospheric models and measurement techniques, these will surely decrease.

A new section (Sect. 3.4) has been added to discuss the uncertainties of local measurements, PBLH, wet deposition and trajectory calculation. Uncertainties induced by the local measurements are rather low for CO, for BC, uncertainties are below 12%. In the evaluation of the uncertainties introduces by the modelled PBLH values, we found out that the PBLH mostly influences the calculation result of the C_l. Overestimating (underestimating) PBLH by 1% would result in an variation of the retrieved emission field by 1% (-1%). The uncertainty of the wet deposition ranges from 0 to 21% across the domain. Trajectory displacement errors are mostly within 1.5 times the grid size. More details on the methodology of the uncertainty analyses and according discussions can be found in Sect 2.5 and in Sect.3.4, respectively.

There are several ways for determining which grids to use for updating emission inventories. You may filter them based on sample number in each grid or according to distance to receptor point (due to trajectory position errors). These discussions are not within the scope of our work and will not be discussed in the revised manuscript.